Crystal Structure of the C-terminal Domain of the Two-Component System Transmitter Protein Nitrogen Regulator II (NRII; NtrB), Regulator of Nitrogen Assimilation in *Escherichia coli*[†,‡]

Yuanda Song,[§,||] Daniel Peisach,[§,⊥,||] Augen A. Pioszak,[§] Zhaohui Xu,[§,⊥] and Alexander J. Ninfa*[,§]

Department of Biological Chemistry, University of Michigan Medical School, Ann Arbor, Michigan 48109, and Life Sciences Institute, University of Michigan, Ann Arbor, Michigan 48109

Received November 13, 2003; Revised Manuscript Received March 25, 2004

ABSTRACT: The kinase/phosphatase nitrogen regulator II (NRII, NtrB) is a member of the transmitter protein family of conserved two-component signal transduction systems. The kinase activity of NRII brings about the phosphorylation of the transcription factor nitrogen regulator I (NRI, NtrC), causing the activation of Ntr gene transcription. The phosphatase activity of NRII results in the inactivation of NRI−P. The activities of NRII are regulated by the signal transduction protein encoded by *glnB*, PII protein, which upon binding to NRII inhibits the kinase and activates the phosphatase activity. The C-terminal ATP-binding domain of NRII is required for both the kinase and phosphatase activities and contains the PII binding site. Here, we present the crystal structure of the C-terminal domain of a mutant form of NRII, NRII-Y302N, at 1.6 Å resolution and compare this structure to the analogous domains of other two-component system transmitter proteins. While the C-terminal domain of NRII shares the general tertiary structure seen in CheA, PhoQ, and EnvZ transmitter proteins, it contains a distinct β-hairpin projection that is absent in these related proteins. This projection is near the site of a well-characterized mutation that reduces the binding of PII and near other less-characterized mutations that affect the phosphatase activity of NRII. Sequence alignment suggests that the β-hairpin projection is present in NRII proteins from various organisms, and absent in other transmitter proteins from *Escherichia coli* K-12. This unique structural element in the NRII C-terminal domain may play a role in binding PII or in intramolecular signal transduction.

The two-component signal transduction systems comprise the most common type of signaling system in bacteria and are also found in lower eukaryotes (reviewed in ref *1*). In these signaling systems, phosphorylation and dephosphorylation of a protein receiver domain is used to control the activity of an enzyme or macromolecular complex. In most cases, the receiver domain regulates an associated DNA-binding domain that activates or represses a set of genes when the receiver domain is phosphorylated.

Interestingly, the receiver domain appears to catalyze its own phosphorylation as well as its own dephosphorylation on a highly conserved aspartate residue (*2*, *3*). Both the phosphorylation of the receiver and its dephosphorylation are facilitated by a partner known as the transmitter protein (*4*). The transmitter protein brings about the phosphorylation of the receiver domain (kinase activity) by binding ATP and phosphorylating itself on a highly conserved histidine residue (*2*, *5*, *6*); phosphoryl groups are then transferred from the phospho-histidine to the receiver aspartate (*2*, *7*). The autophosphorylation of the transmitter occurs by a trans-intramolecular mechanism, in which ATP bound to the C-terminal domain of one subunit of the dimeric transmitter protein phosphorylates the highly conserved histidine within the central domain of the opposing subunit of the dimer (*8*). Two observations suggest that the receiver catalyzes the phosphotransfer step: a peptide containing the phosphorylated histidine from the CheA transmitter could be used to phosphorylate the CheY receiver (*2*), and in some cases, such as the NRI/NRII[1] and Che systems, small molecule phosphorylated intermediates, such as acetyl phosphate, may serve as the phosphoryl group donor for receiver phosphorylation independent of the transmitter protein (reviewed in ref *9*).

The phosphorylated receiver proteins have variable stability, representing a variable "autophosphatase" activity (e.g., ref *3*). For the transmitter-mediated dephosphorylation reaction, it has not been resolved whether the transmitter protein acts catalytically as a phosphatase or whether it acts to

[†] This work was supported by Grant GM-59637 from the NIH-NIGMS.

[‡] Coordinates for the CTD of NRII have been deposited in the Protein Data Bank as entry 1R62.

* To whom correspondence should be addressed. Mailing address: Department of Biological Chemistry, University of Michigan Medical School, 1301 East Catherine, Ann Arbor, MI 48109-0606. Phone: 734 763-8065. Fax: 734 763-4982. E-mail: aninfa@umich.edu.

[§] University of Michigan Medical School.

[⊥] University of Michigan.

[||] Both authors contributed equally to this work and are considered co-first authors.

[1] Abbreviations: NRI, nitrogen regulator I; NtrC, enhancer-binding transcription factor that is controlled by phosphorylation/dephosphorylation; NRII, nitrogen regulator II; NtrB, kinase/phosphatase for NRI; PII, Signal transduction protein encoded by *glnB*, regulator of NRII activities; CTD, C-terminal domain of NRII, site of ATP binding and PII binding; DTT, dithiothreitol.

10.1021/bi049474r CCC: $27.50
Published on Web 05/05/2004

increase the rate of the receiver autophosphatase actvity. We refer to this activity as the transmitter phosphatase activity. For regulation, depending on the system the autophosphorylation of the transmitter, the phosphatase activity of the transmitter, or both activities may be controlled. Different systems may respond to intracellular or extracellular signals that act directly on the conserved domains or on associated domains that are cytoplasmic or project through the membrane and into the periplasm or extracellular space. In more complex two-component signaling systems, multiple transmitter and receiver modules may be incorporated into complex phospho-relay systems that may include other types of phosphotransfer domains and unrelated phosphatase activities (*10*).

The receiver and transmitter proteins of the two-component systems are easily recognized by the presence of conserved amino acid sequences (reviewed in ref *11*). Receiver proteins are recognized by the presence of a highly conserved receiver domain of about 120 amino acids. The transmitter conserved sequences, which are typically about 230 amino acids, form two domains: a four-helix bundle dimerization and phosphotransferase domain (referred to as a DHP domain, or "domain A") and a C-terminal ATP binding domain (referred to as "domain B"). The four-helix bundle contains the major dimerization determinants, the site of histidine phosphorylation, and amino acids involved in the phosphatase activity. In CheA and a subset of the transmitter proteins, the site of autophosphorylation is on a separate N-terminal domain (distinct from the dimerization domain). The C-terminal ATP-binding domain, which is distantly related to the ATP-binding domain of gyrase and HSP90 proteins (*12*), is involved in both kinase and phosphatase activities. In most transmitter proteins, unrelated domains are found at the N-terminus of the protein, while in a minority of cases unrelated domains are found at the C-terminus. These unrelated domains are inferred to play a role in sensation, signal transduction, or cellular localization. In some cases, the transmitter and receiver domains may be present in a single protein.

The NRII/NRI (NtrB/NtrC) two-component system controls the expression of nitrogen-regulated Ntr genes in *Escherichia coli* and related bacteria (reviewed in ref *13*). It is among the simplest of two-component systems with both transmitter (NRII) and receiver (NRI) being cytoplasmic proteins. The regulation of the kinase and phosphatase activities of the transmitter NRII are understood in some detail. The binding of the PII signal transduction protein to the C-terminal ATP-binding domain of NRII activates its phosphatase activity and inhibits its kinase activity (*3*, *4*, *14*−*16*). The availability of PII for this interaction is controlled by reversible covalent modification (uridylylation) of PII catalyzed by the glutamine-controlled uridylyl transferase/uridylyl removing enzyme (UTase/UR) and by allosteric control of PII by small molecule effectors (primarily α-ketoglutarate) that reflect the cellular carbon and nitrogen status (reviewed in ref *13*).

Sequence comparison of NRII to related proteins, structural information from related proteins (*12*, *18*−*20*), genetic studies of NRII (*17*, *21*, *22*), and studies of the properties and activities of polypeptides derived from NRII (*14*) suggest that NRII is organized into three domains, as depicted in Figure 1. The interactions of the N-terminal domains are not

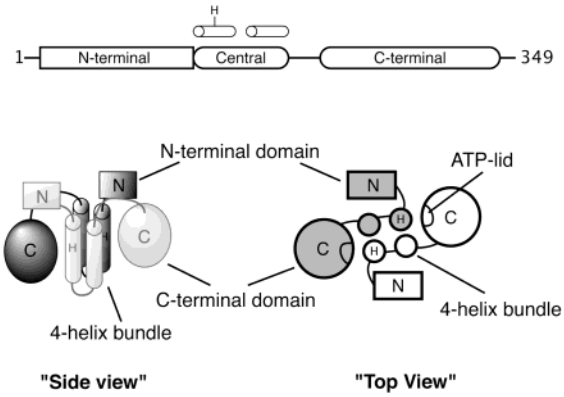

FIGURE 1: The proposed domain organization of NRII. NRII contains three domains: the N-terminal domain, a central dimerization domain that forms a four-helix bundle, and an ATP binding C-terminal domain. In the lower portion of the figure, one subunit of the homodimer is drawn in white or light gray, the other in dark gray. H denotes the histidine that becomes autophosphorylated.

understood. The N-terminal domain of NRII contains a PAS motif, which in other proteins has been found to be involved in binding regulatory ligands or in intramolecular and intermolecular domain interactions (*23*). The isolated N-terminal domain behaves as a monomer in solution (*14*). The central domain of the dimer consists of a four-helix bundle, two helices contributed by each monomer. When the central domain is expressed as a fusion with the monomeric maltose-binding protein (MBP), the fusion protein is a dimer that can be phosphorylated in a PII-regulated fashion by the isolated C-terminal domain of NRII (*14*). The purified central domain also displays weak phosphatase activity that is not regulated by PII (*14*). The C-terminal domain of NRII contains the ATP and PII binding sites. As is often seen in ATP binding proteins, structures of histidine kinases and related ATP-binding proteins (gyrase, HSP90) with bound nucleotide show an extended helix containing loop that forms a lid over the ATP (*12*). Cross-linking studies show that the phosphatase complex consists of a single PII trimer bound to one of the C-terminal domains of the NRII dimer (*15*).

All of the domains of NRII appear to collaborate in the kinase and phosphatase activities and operate in a coordinated fashion. Much like a two-stroke engine, the autophosphorylation of NRII occurs by an apparent half-of-the-sites mechanism. This results from a 70-fold difference in the equilibrium constants for the phosphorylation of the first and second of the two histidine autophosphorylation sites in the dimer (*24*). Furthermore, the doubly phosphorylated dimer is unstable and rapidly decays to the hemiphosphorylated form. This asymmetry is relaxed by removal of either the N-terminal domains or one of the C-terminal domains of the NRII dimer, and these changes also destroy the phosphatase activity of NRII (*24*). Furthermore, mutations affecting the phosphatase activity can be found in all domains of NRII (*17*).

Genetic and biochemical studies of the PII-activated phosphatase activity of NRII indicate that two distinct surfaces of the C-terminal domain are involved, as identified by clusters of mutations that reduce the activity (*17*). One of these mutation clusters maps to a site deduced to be part of the ATP lid over the ATP binding site on the basis of the structures of related proteins (*18*, *20*, *21*). The other cluster of mutations maps to the opposite side of the domain and

may define the PII binding site. One mutant protein from this cluster, the S227R protein, was shown to be severely defective in binding PII. In contrast, mutant proteins altered in other parts of NRII were severely defective in the phosphatase activity yet retained the ability to bind to PII (*17*).

Biochemical studies of the PII-activated phosphatase activity of NRII provide a clue as to how the domains of NRII collaborate in the PII-activated phosphatase activity. Specifically, experiments with heterodimeric mutant proteins formed in vitro were only consistent with a model where the two C-terminal domains of NRII play distinct roles. One of the NRII C-terminal domains binds PII, while the CTD ATP lid of the opposing subunit collaborates with the central domain to maintain the "phosphatase" conformation or participates directly in the reaction (*25*).

Although the full-length NRII is a cytoplasmic protein, it is relatively insoluble, not easily purified, and has proven difficult to crystallize (unpublished data). This behavior is shared by the isolated CTD of NRII, suggesting that these properties of the full-length protein are largely due to the CTD. Here, we screened an existing set of mutant forms of NRII and observed that the Y302N mutation resulted in improved solubility of the full-length protein and the isolated CTD. We observed that the purified NRII-Y302N-CTD was active as a kinase and that this activity was regulated by PII as is the case with wild-type NRII. We also found that the NRII-Y302N-CTD forms a stable complex with PII that could be readily detected by gel-filtration chromatography. Most importantly, the NRII-Y302N-CTD was able to produce diffraction quality crystals from which we could solve the structure. The ATP lid of the domain is unobservable and assumed to be disordered in our structure, but our structure is well defined in the region where the S227R mutation described above affects the binding of PII. Interestingly, this portion of the domain structure differs from related transmitter protein domains that are not regulated by PII, and thus the differences may reflect features required for the binding of PII or intramolecular signal transduction of the signal provided by PII binding.

MATERIALS AND METHODS

Overexpression and Purification of the NRII C-Terminal Domain (CTD). The CTD (residues 190−349) of wild-type NRII and NRII-Y302N were amplified by PCR as described previously (*14*) and cloned into the vector pSJ4, a derivative of pET30a (Novagen). Cloning used the *Nde*I and *Eco*RI restriction sites of pSJ4, resulting in a polyhistidine (eight histidines) tag being present at the N-terminus of the CTD. CTD was overexpressed in *E. coli* strain BL21(DE3) induced with 0.4 mM isopropyl-β-D-thiogalactopyranoside (IPTG). For purification, cells were lysed by sonication, and the cellular debris was removed by centrifugation. The clarified extract was then loaded onto a 20 mL Ni^{2+}-NTA column equilibrated with buffer A [50 mM Tris-HCl, pH 7.5, 200 mM KCl, 20 mM β-mercaptoethanol, 10 mM imidazole, 10% (v/v) glycerol] and eluted with a gradient of 10−250 mM imidazole in buffer A. Fractions were assayed by SDS−PAGE, and the peak fractions were combined, concentrated by ammonium sulfate precipitation, resuspended in buffer B [50 mM Tris-HCl, pH 7.5, 200 mM KCl, 20 mM β-mercaptoethanol, 10% (v/v) glycerol] and further purified by gel filtration chromatography on a Sephadex G-75 column equilibrated in buffer B. Fractions containing the CTD were again identified by SDS−PAGE, pooled, dialyzed into storage buffer [50 mM Tris-HCl, pH 7.5, 200 mM KCl, 50% (v/v) glycerol], and stored in aliquots at −80 °C. Proteins were greater than 90% pure as estimated by SDS−PAGE.

To remove the polyhistidine tag, purified CTD was cleaved with histidine-tagged TEV protease (Invitrogen), and the CTD was separated from the cleaved histidine tag and the protease by passage through a Ni^{2+}-NTA column. Selenomethionine-substituted CTD was produced using B834(DE3) cells and purified by the same methods.

Transphosphorylation Assay. The ability of the purified CTD to bring about the phosphorylation of a fusion protein consisting of maltose-binding protein linked to the central (DHP) domain of NRII was assayed as described previously (*14*).

Interaction of PII with CTD. To test whether the CTD interacts with PII, a gel filtration assay using Sephadex G-75 (36 mL column) was employed. The column was equilibrated in G75 buffer [50 mM Tris-HCl, pH 7.5, 200 mM KCl, 10% (v/v) glycerol] containing or lacking $MgCl_2$ (10 mM), ATP (0.5 mM), and α-ketoglutarate (50 μM). PII was purified as previously described (*15*). Samples (500 μL) containing either 2 mg of purified PII (106 μM), 0.95 mg of CTD (106 μM), or a mixture of both proteins were fractionated, and fractions were assessed by SDS−PAGE. Under these conditions, NRII-CTD and PII elute from the column at distinct volumes, reflecting their difference in mass. When cochromatographed in the presence of Mg-ATP and α-ketoglutarate, the two proteins coeluted, reflecting formation of a complex.

Testing the Solubility of NRII Mutant Proteins. For this test, the pJLA503 expression system was used, as described previously (*17*). Proteins were induced by shifting the temperature from 30 to 44 °C for 4 h, after which cells were pelleted, resuspended in lysis buffer [50 mM Tris-HCl, pH 7.5, 1 mM DTT, 10% (v/v) glycerol] containing either 50 or 300 mM KCl, and disrupted by sonication. The disrupted cells were either mixed with SDS−PAGE loading buffer or clarified by centrifugation and then mixed with SDS−PAGE loading buffer. The samples were then heated at 95 °C for 10 min and subjected to SDS−PAGE; comparison of the two samples revealed whether sonication in the presence of high concentration of KCl resulted in loss of the NRII protein from the soluble fraction. For wild-type NRII, greater than 50% of the protein was lost from the soluble fraction after sonication in the presence of 300 mM KCl.

Structure Determination. The structure was first determined using the multiple wavelength anomalous diffraction (MAD) method with selenium as the anomalous scattering atoms and later refined against a 1.6 Å resolution native data set (*26*). Diffraction quality crystals were grown by the sitting drop method using native and selenomethionine-substituted proteins that had been cleaved with the TEV protease to remove the histidine tag. Two microliters of 5 mg/mL CTD of NRII (determined by the Bradford assay) in 10 mM Tris-HCl, pH 7.5, was mixed with 2 μL of mother liquor containing 5% PEG 20 000, 0.1 M MES, pH 6.1, and equilibrated over 1 mL of mother liquor at 23 °C. CTD crystals appeared overnight and grew to optimal size ($0.2 \times 0.2 \times 0.6$ mm^3) within one week. Crystals were cryoprotected

Table 1: Crystallographic Data Statistics

Data Collection Statistics

crystal	space group	cell dimensions
native	C2	$a = 96.4$ Å, $b = 32.9$ Å, $c = 46.0$ Å, $\beta = 108.2°$
SeMet	C2	$a = 96.4$ Å, $b = 32.9$ Å, $c = 46.0$ Å, $\beta = 108.3°$

dataset	d_{min} (Å)	no. of meas.	no. of unique reflns	completeness (%)[a]	I/σ[a]	R_{sym} (%)[a,b]
native	1.6	73 198	18 060	98.8 (95.3)	35 (4.2)	3.9 (19.8)
SeMet $\lambda1$ (0.9784 Å)	1.9	64 589	10 486	99.0 (99.9)	34 (10.4)	5.5 (15.9)
SeMet $\lambda2$ (0.9786 Å)	1.9	64 387	10 488	99.1 (100.0)	35 (10.2)	5.7 (15.9)
SeMet $\lambda3$ (0.9559 Å)	1.9	63 733	10 494	98.9 (99.2)	32 (6.4)	5.6 (21.8)
SeMet $\lambda4$ (1.0023 Å)	1.9	63 757	10 497	99.0 (99.6)	35 (8.4)	5.2 (18.8)

figure of merit vs resolution after SOLVE

D_{min}	total	6.99	4.48	3.53	3.00	2.65	2.41	2.22	2.06
no. of reflns	9327	461	775	989	1163	1293	1428	1564	1654
FOM	0.50	0.74	0.64	0.63	0.63	0.56	0.48	0.38	0.28

figure of merit vs resolution after RESOLVE

D_{min}	total	5.7	3.6	2.9	2.5	2.1	2.0
no. of reflns	9327	390	1270	1573	1582	2791	1721
FOM	0.63	0.93	0.91	0.82	0.68	0.51	0.32

Refinement Statistics (Native Dataset)

number of reflections (working/test)	15 907/1742
number of non-hydrogen atoms	1062
number of water molecules	109
resolution (Å)	27.6−1.6
R_{cryst}/R_{free} (%)[c]	23.7/24.6
bond length deviation (Å)	0.005
bond angle deviation (deg)	1.3
average *B*-factor of model (Å^2)	26.2
*B*_overall (by Patterson) (Å^2)	26.3
optical resolution (Å)	1.41
estimated minimal error (Å)	0.039
estimated maximal error (Å)	0.277
Matthews coefficient	2.12
corresponding solvent %	41.4

[a] Values in parentheses are for the highest resolution bin. [b] $R_{sym} = \sum_h\sum_i|I_i(h) - \langle I(h)\rangle|/\sum_h\langle I(h)\rangle$, where $I_i(h)$ is the ith measurement and $\langle I(h)\rangle$ is the weighted mean of all measurements of $I(h)$. [c] $R = \sum(|F_o| - K|F_c|)/\sum|F_o|$. R_{free} is the *R*-value obtained for a test set of reflections that consisted of a randomly selected 10% subset of the diffraction data used during refinement of σ_A value calculations.

by immersion for 1 min in 12% PEG 20 000, 20% (v/v) ethylene glycol, 0.1 M MES, pH 6.1, followed by flash cooling in liquid nitrogen. The crystals belonged to the monoclinic space group *C*2, had unit cell dimensions $a = 96.4$ Å, $b = 32.9$ Å, $c = 46.0$ Å, and $\beta = 108.2°$, and contained one molecule of the CTD of NRII per asymmetric unit. A 1.9 Å four-wavelength MAD data set from a selenomethionine crystal was collected at the SBC-CAT beamline 19-ID at the Advanced Photon Source and processed using the HKL2000 package (*26*, *27*). A 1.6 Å native data set was collected at the DND-CAT beamline 5-ID at the Advanced Photon Source and processed with DENZO and SCALEPACK (*27*).

There are two expected selenium sites (methionine residues) in the CTD, but only one of these was identified (the other is located in a loop that is unobserved and assumed to be disordered) using the SOLVE package (*28*). Phases were subsequently improved by density modification with RESOLVE (*29*, *30*). The high-quality map obtained allowed unambiguous tracing of 102 residues of the CTD in four segments by RESOLVE. All subsequent refinement was performed against a 1.6 Å native data set using the program CNS (*31*). Progress was measured by cross-validation (R_{free} calculation) with a 10% randomly selected test set. Initial refinement was performed with data to 2.0 Å resolution and consisted of several iterations of conjugated gradient minimization, grouped *B*-factor refinement, and torsion angle dynamics simulated annealing using the maximum likelihood target function (MLF), followed by model rebuilding in the program O (*32*). Once the model was completely built to 132 residues, all the data from 30 to 1.6 Å was used with individual atomic *B*-factors refined. The final model includes residues 194−292, residues 313−349, and a total of 109 water molecules. Residues 190−193 and 293−312 are not visible and assumed to be disordered. Atomic coordinates

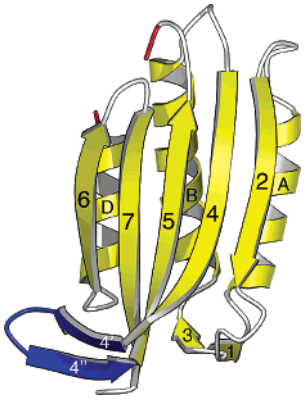

FIGURE 2: A ribbon model of the crystal structure of the Y302N-CTD of NRII. The β-hairpin uniquely found in NRII is colored blue. The residues bordering the missing ATP binding site lid are red.

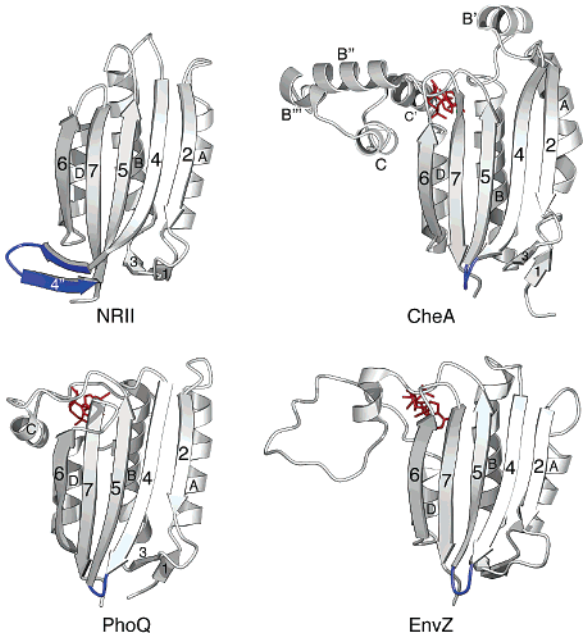

FIGURE 3: Structure comparison of the CTD of NRII with related domains from CheA, PhoQ, and EnvZ. Ribbon diagrams of the CTD of NRII (PDB accession code 1R62), PhoQ (PDB accession code 1ID0), EnvZ (PDB accession code 1BXD) and CheA (PDB accession code 1I58) ar compared. The loops or β-hairpin connecting strands 4 and 5 are blue. The nucleotide (where observed) is colored red.

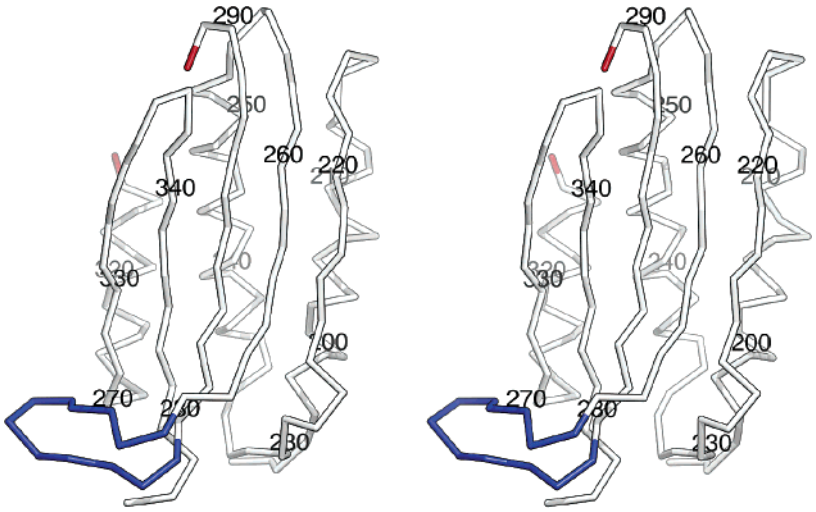

FIGURE 4: A stereo Cα trace of the CTD with every 10th amino acid numbered. The β-hairpin connecting strands 4 and 5 is blue. Red denotes the beginning and end of the missing ATP lid.

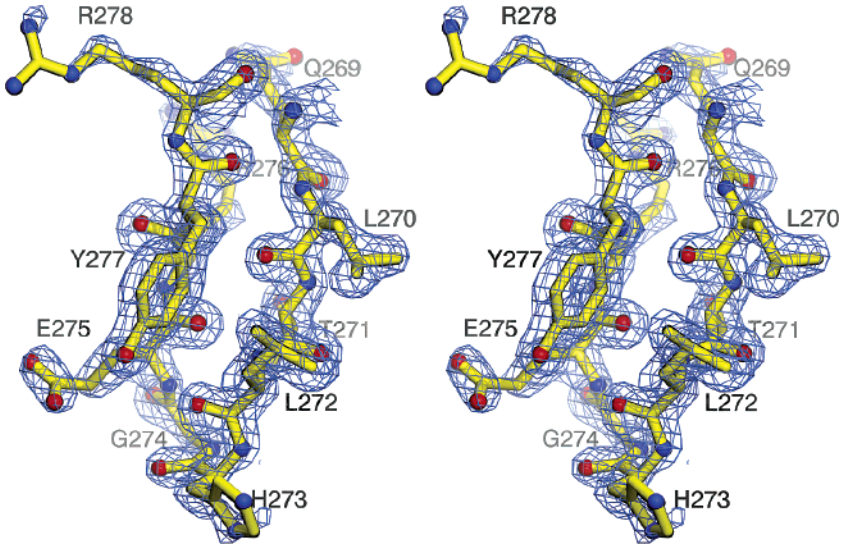

FIGURE 5: Electron density observed for the β-hairpin. A stereoview of a simulated annealing composite omit (unbiased) $2F_o - F_c$ electron density map contoured at 1.5σ and superimposed upon the final model of the β-hairpin between strands 4 and 5 in NRII is shown.

and structure factors have been deposited into the Protein Data Bank (accession code 1R62). Final analysis of the atomic coordinates was performed in the program SFCHECK, which is a part of the CCP4 package (*33*).

Figure Preparation. Molscript (*34*), POVSCRIPT (*35*) and POV-ray (http://www.povray.org) were used to produce Figures 2−6. Grasp (*36*) was used to produce Figure 6.

RESULTS AND DISCUSSION

Identification of a Full-Length NRII Protein with Increased Solubility. Although wild-type NRII expresses well, the protein was prone to aggregation at high concentration and readily precipitated during crystallization trials. To overcome this problem, we screened an existing collection of mutant forms of NRII for proteins that remained in the supernatant fraction after sonication in 300 mM KCl and centrifugation. The D225V, S227I, S227R, L228R and P303T proteins (with alterations in the CTD) were less-soluble than was the wild-type protein, S227R being the most soluble of the group. The I12F, L16R, A35V, and L83P proteins (with alterations in the N-terminal domain) also displayed poor solubility, with L16R being the most soluble of the group (data not shown). For each of these proteins, the fraction remaining in the supernatant after cell disruption ranged from 10% to 20% for the mutants and approximately 40% for the wild-type enzyme. The Y302N protein uniquely displayed improved solubility over the wild-type protein; essentially all the protein remained in the supernatant fraction after cell sonication in 300 mM KCl. The results of these experiments dictated the choices of proteins that were analyzed in the published enzymological studies (*17*, *25*). The Y302N protein had slightly higher kinase activity than wild-type NRII, but was severely defective in PII-activated phosphatase activity (*17*). Nevertheless, the mutant protein was observed to bind to PII nearly as well as does wild-type NRII (*17*).

Purification of the NRII-Y302N-CTD. Attempts to crystallize the full-length NRII-Y302N only gave rise to poorly diffracting crystals (to 6 Å resolution), so we attempted to crystallize its CTD alone. The Y302N-CTD was overexpressed as a fusion with an N-terminal His tag and TEV protease cleavage site. The fusion protein was purified by affinity chromatography and gel-filtration chromatography.

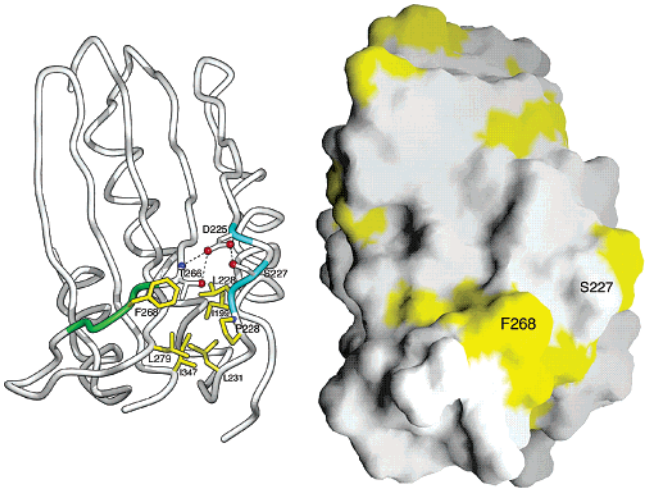

FIGURE 6: The potential PII interaction surface. A Cα trace (left) and a solvent-accessible surface (right) of the CTD drawn in the same orientation are presented. On the left panel, the backbone trace is colored green for residues 267−270 and cyan for residues 225, 227, and 228. Mutations at these residues reduce the phosphatase activity of NRII. Hydrophobic side chains are colored yellow. On the right panel, the surface is colored yellow where it is formed by hydrophobic side chains.

Aliquots of the purified fusion protein were cleaved with His-tagged TEV protease, and the CTD was purified from the cleavage reaction mixtures by passage through the affinity resin. Owing to the details of its construction, this purified domain contained three additional amino acids (glycine-serine-histidine) at its N-terminus.

The binding of PII to the CTD was analyzed by gel filtration chromatography on Sephadex G-75. Prior studies had shown that the binding of PII to NRII is observed only in the presence of Mg^{2+}, ATP, and α-ketoglutarate and that for optimal interaction the concentration of free α-ketoglutarate must be between 20 and 200 μM (*15*). In the presence of these ligands at the appropriate concentrations, PII and the CTD when chromatographed separately eluted from the gel filtration column at distinct volumes reflecting their different molecular mass, while an equimolar mixture of PII and CTD coeluted from the column in a complex with mass somewhat larger than PII and considerably larger than CTD (data not shown). Under the conditions used, essentially all of the CTD and PII appeared to be in the complex. In the absence of the small molecule ligands, there was no evidence of complex formation between PII and the CTD (data not shown). These results indicate that the purified Y302N-CTD retained the ability to bind tightly to PII.

We verified that our preparation of Y302N-CTD was active in bringing about the phosphorylation of the isolated central domain of NRII (transphosphorylation activity). For this experiment, the wild-type dimeric central domain of NRII was provided as a fusion to the maltose-binding protein, as before (*14*). The CTD brought about the phosphorylation of the NRII central domain, and this activity was strongly inhibited by PII (data not shown). However, the specific activity of the Y302N-CTD was about half that of the wild-type CTD in the transphosphorylation assay (data not shown).

The Crystal Structure of the CTD of NRII. We crystallized the Y302N-CTD and determined its structure. The data and refinement statistics are summarized in Table 1. As illustrated in Figure 2, the core of the NRII-CTD contains an α/β sandwich fold consisting of a five-stranded mixed β sheet (strands 2, 4, 5, 6, and 7) packed against three amphipathic α helices (A, B, and D). One end of this core contains a long stretch of unobserved residues connecting strand 5 and helix D (residues 293−312), which forms the ATP binding site. The other end of the core is closed by a short β-sheet composed of strands 1 and 3. Between strands 4 and 5, a short β-hairpin consisting of β strands 4′ and 4″ is observed. Strand 4′ packs against the loop connecting helix D and strand 6. According to a Ramachandran analysis of the protein, 96.5% of the residues are in most favorable conformations and 3.5% are in additional allowed conformations. None of the residues are in generously allowed or disallowed conformations.

A comparison of the NRII-CTD structure to the analogous domains from the related EnvZ, CheA, and PhoQ transmitter proteins (involved in porin gene regulation, chemotaxis, and virulence, respectively) is shown in Figure 3 (*12*, *18*, *20*). The RMSD for the α-carbon atoms in this core between NRII and EnvZ, CheA, and PhoQ are 1.9, 1.3, and 1.3 $Å^2$, respectively.

The structure of NRII did not contain an observable ATP lid. This region was also disordered in the EnvZ NMR structure. In the PhoQ and CheA structures, the ATP lid and nucleotide were well defined and the region contained a helix (helix C). To match the nomenclature of these other structures, we designated the three helices in the NRII-CTD structure A, B, and D. Attempts to cocrystallize the NRII-CTD with non-hydrolyzable ATP analogues gave rise to crystals that belonged to a different space group but still had no observable nucleotide. However, due to the similarity to the related structures we believe the ATP binding site to be enclosed by a flexible lid that is inserted between strand 5 and helix D. Mutational studies have suggested that this region of NRII is indeed involved in ATP binding (*22*).

A new feature of the NRII-CTD structure is the β-hairpin located between strands 4 and 5 (Figure 2, Figure 3). This forms a projection from the surface of the CTD that is missing in the other transmitter proteins. In its place, the other transmitter proteins have a short turn that connects strands 4 and 5 (Figure 3). A stereoview of the backbone structure of the NRII-CTD is provided along with a stereoview of the density fit for the unique β-hairpin of the NRII-CTD (Figures 4 and 5). This portion of the NRII-CTD is well defined in our structural model. Given the similarity of the core of the CTD structures and the close apposition of the ends of the β-hairpin of NRII, it is likely that this element arose by a short insertion into the structurally conserved core domain.

The β-Hairpin of the NRII-CTD May Be Involved in PII Binding. Mutations of NRII in the ATP lid, in both helices of the central domain, and throughout the N-terminal domain can diminish the PII-activated phosphatase activity. The most soluble of these proteins were analyzed, indicating that they did not result in a significant defect in the binding of PII (*17*). Similarly, several mutations that lie in the vicinity of the β-hairpin element of the NRII-CTD dramatically reduce the PII-activated phosphatase activity of NRII. This set includes three different mutations at position S227, mutations at positions D225 and L228, and a mutation that deletes residues 267−270 (AFQL, forming the first part of strand 4′ that is part of the novel β-hairpin projection). Of these,

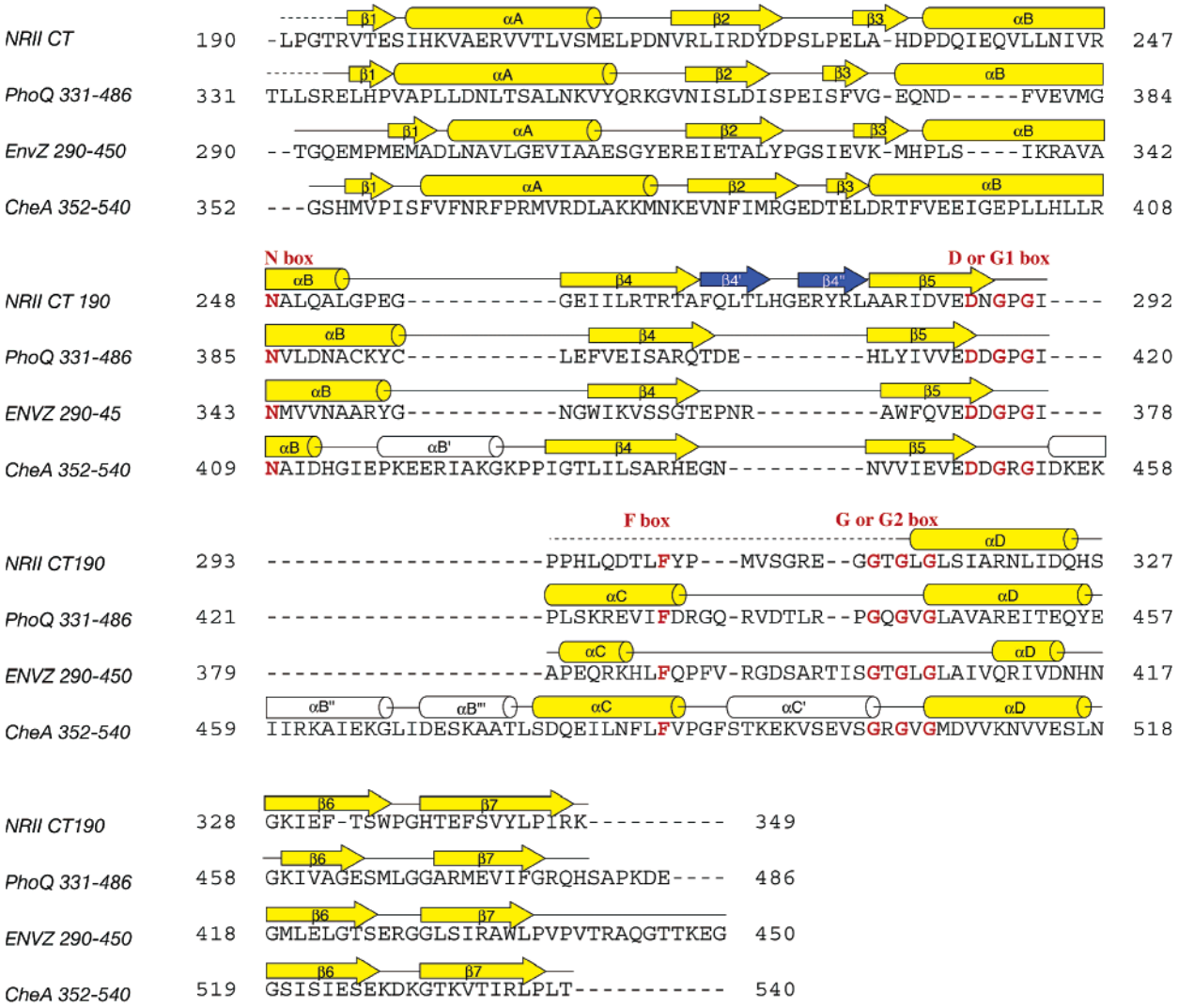

FIGURE 7: Alignment of the ATP-binding domains of transmitter proteins with known structures. The sequences of the ATP-binding domains of NRII, PhoQ, EnvZ, and CheA were initially aligned by the program ClustalW (*39*) and then adjusted by hand to align the secondary structural elements observed in the NMR and crystal structures. Secondary structure elements are indicated above the sequences: α-helices are drawn as cylinders, β-strands as arrows, other elements as solid lines, and structurally unobserved residues at the N-terminus and in the mid-sequence as dashed lines. Helices and strands from the conserved CTD core are colored yellow. The additional β-hairpin in NRII is drawn in blue. Additional helices observed in CheA crystal structure are colored white. Highly conserved residues from the proposed ATP binding site are indicated with red letters.

the S227R protein was the most soluble, and analysis of this protein indicated that it was severely defective in binding PII, contrary to what was seen with the changes in other parts of NRII (*17*). Presumably the other mutations in this region of the protein also affect the binding of PII.

As shown in Figure 6, there is a hydrophobic surface on NRII made up of residues from the β-hairpin and from the opposing loop found between strands 2 and 3. The hydrophobic surface in this portion of the domain forms a shallow groove that could interact with another protein. The presence of mutations diminishing the phosphatase activity and an appropriately hydrophobic patch raised the possibility that this is the PII-binding site. Another possible explanation of the role of the side chains mentioned above is that they stabilize the position of the β-hairpin element, allowing PII recognition and binding. The β-hairpin appears to be held in place by a hydrogen bond network formed between the side chains of S227 and D225 and the side chain and backbone amide of T266. Mutations of any of these residues could displace the β-hairpin. The L228 side chain projects into the hydrophobic core; its mutation to arginine (*17*) could disrupt the structure of the β-hairpin as well. Thus, these mutations may not define contacts directly but instead exert indirect effects by altering the β-hairpin position. In summary, the PII binding site may consist of the hydrophobic patch, the β-hairpin element, or a combination of both.

How Does PII Binding to the CTD Regulate the Kinase and Phosphatase Activities? A reasonable hypothesis for the regulation of NRII kinase and phosphatase activities by PII is that the binding of PII affects the conformation of the ATP lid. The ATP lid is implicated in both the kinase and phosphatase activities of NRII, as revealed by the effects of mutations in this part of the protein (*17*, *22*, *37*). Furthermore, ATP is an activator of the phosphatase activity of NRII (*3*, *14*). The Y302N, P303L, and P303T mutations in the ATP lid cause a severe and specific defect in the phosphatase activity in vivo, and the purified Y302N protein was shown to be specifically defective in the phosphatase activity yet retained the ability to bind to PII (*17*). In light of all the available data for NRII and the related transmitter proteins,

it seems likely that the ATP lid of the CTD is close to and interacts with the active site histidine-containing region (H-box) of the central domain containing the site of autophosphorylation and where numerous mutations affecting the phosphatase activity of NRII (*21*) and other transmitters map. Furthermore, recent enzymological studies suggest that the two CTDs of the NRII dimer play two distinct roles in the phosphatase activity, suggesting that the ATP lids have different conformations corresponding to different functional activities (*38*).

With this in mind, it is important to understand how the binding of PII to a distant surface of the CTD regulates the structure of the ATP lid. A reasonable scenario, albeit a speculative one, is raised by our structural data. Specifically, helix D has a minimal number of interactions with other parts of the molecule. This is because it points away from the core β-sheet and lies at an angle to helix B. Helices B and D have a single hydrophobic interaction where they cross one another via residue V241 of helix B and residues I318 and A319 of helix D. Helix D also has minimal interactions with strands 6 and 7. Specifically, I330 in helix D interacts with side chains of R320 and I323 in strand 6, and L316 in helix D weakly interacts with F341 in strand 7. Because of the limited interactions between helix D and the rest of the domain, helix D may display a scissors-like or sliding motion relative to helix B. This may also be true for PhoQ, which like NRII shows limited interactions between helix D and the rest of the domain. Strand 4′ of the β-hairpin in NRII displays multiple interactions with the loop connecting strand 6 and helix D. Movement of strand 4′ (brought about by PII binding) could be transmitted to the ATP lid by altering the position of helix D. A comparison of the structures of a complex of NRII and PII versus the structure of NRII alone would answer this question.

Alternatively, PII could bind in a bidentate fashion to NRII, interacting with both the β-hairpin and the ATP lid. A similar regulatory mechanism is seen with CheA. The CheA transmitter protein is regulated by interaction with the chemotactic receptors and CheW adaptor protein. These interactions utilize a novel regulatory domain (P5) of CheA that lies after the ATP-binding domain. The P5 domain is large enough to interact with the kinase domain of CheA at two locations: one is roughly at the same location as the β-hairpin in NRII; the other is the ATP lid itself. In addition, CheA has a more extensive set of interactions between helices B and D. In CheA, helix B is longer and has hydrophobic interactions with helix D at both its middle and N-terminal end, while NRII has a shorter helix B that does not form until after P235. On the basis of the binding positions of the regulatory P5 domain and the more rigid arrangement of helices B and D, it seems unlikely that CheA would utilize a helix D motion-dependent mechanism for control of the ATP lid conformation. More likely, the P5 domain of CheA may directly control the ATP lid conformation.

The β-Hairpin Element is a Distinctive Feature of NRII Proteins. Since the NRII-CTD structure reveals a β-hairpin element and is regulated by PII, we compared the structures of the CTD of two-component regulatory system transmitter proteins to discern whether any others are likely to contain a similar structural element and are likely also to be regulated by PII. An alignment of the four domains for which structural information is available clearly shows that PhoQ, EnvZ, and CheA lack the β-hairpin element found in NRII (Figure 7). None of the two-component systems of *E. coli* K-12 appear to contain this β-hairpin, while the NRII sequences from various organisms all appear to contain the element (not shown). Thus, the β-hairpin seems to be specific to NRII proteins. Further, it is unlikely that PII plays a role in controlling other two-component systems in *E. coli* K-12.

ACKNOWLEDGMENT

The authors thank Ray Trievel and Jack Peisach for constructive criticism of the manuscript.

REFERENCES

1. Stock, A. M., Robinson, V. L., and Goudreau, P. N. (2000) Two-component signal transduction, *Annu. Rev. Biochem. 69*, 183−215.
2. Hess, J. F., Bourret, R. B., and Simon, M. I. (1988) Histidine phosphorylation and phosphoryl group transfer in bacterial chemotaxis, *Nature 336*, 139−143.
3. Keener, J., and Kustu, S. (1988) Proten kinase and phosphoprotein phosphatase activities of nitrogen regulatory proteins NTRB and NTRC of enteric bacteria: roles of conserved amino terminal domain of NTRC. *Proc. Natl. Acad. Sci. U.S.A. 85*, 4976−4980.
4. Ninfa, A. J., and Magasanik, B. (1986) Covalent modification of the *glnG* product, NRI, by the *glnL* product, NRII, regulates the transcription of the *glnALG* operon of *Escherichia coli*, *Proc. Natl. Acad. Sci. U.S.A. 83*, 5909−5913.
5. Weiss, CV, and Magasanik, B. (1988) Phosphorylation of nitrogen regulator I (NRI) of *Escherichia coli*, *Proc. Natl. Acad. Sci. U.S.A. 85*, 8919−8923.
6. Ninfa, A. J., and Bennett, R. L. (1991) Identification of the site of autophosphorylation of the bacterial protein kinase/phosphatase NRII, *J. Biol. Chem. 266*, 6888−6893.
7. Sanders, D. A., Gillece-Castro, B. L., Burlingame, A. L., and Koshland, D. E., Jr. (1992) Phosphorylation site of NtrC, a protein phosphatase whose covalent intermediate activates transcription, *J. Bacteriol. 174*, 5117−5122.
8. Ninfa, E. G., Atkinson, M. R., Kamberov, E. S., and Ninfa, A. J. (1993) Mechanism of autophosphorylation of *Escherichia coli* NRII: trans-phosphorylation between subunits, *J. Bacteriol. 175*, 7024−7032.
9. McCleary, W. R., Stock, J. B., and Ninfa, A. J. (1993) Is acetyl phosphate a global signal in *Escherichia coli*? *J. Bacteriol. 175*, 2793−2798.
10. Appelby, J. L., Parkinson, J. S., and Bourret, R. B. (1996) Signal transduction via the multistep phosphorelay: not necessarily a road less traveled, *Cell 86*, 845−848.
11. Grebe, T. W., and Stock, J. B. (1999) The histidine protein kinase superfamily, *Adv. Microb. Phys. 41*, 139−227.
12. Tanaka, T., Saha, S. K., Tomomori, C., Ishima, R., Liu, D., Tong, K. I., Park, H., Dutta, R., Qin, L., Swindells, M. B., Yamazaki, T., Ono, A. M., Kainosho, M., Inouye, M., and Ikura, M. (1998) NMR structure of the histidine kinase domain of the *E. coli* osmosensor EnvZ, *Nature 396*, 88−92.
13. Ninfa, A. J., Jiang, P., Atkinson, M. R., and Peliska, J. A. (2000) Integration of antagonistic signals in the regulation of bacterial nitrogen assimilation, *Curr. Top. Cell. Regul. 36*, 32−76.
14. Jiang, P., Atkinson, M. R., Srisawat, C., Sun, Q., and Ninfa, A. J. (2000) Functional dissection of the dimerization and enzymatic activities of *Escherichia coli* nitrogen regulator II and their regulation by the PII protein, *Biochemistry 39*, 13433−13449.
15. Pioszak, A. A., Jiang, P., and Ninfa, A. J. (2000) The *Escherichia coli* PII signal transduction protein regulates the activities of the two-component systems transmitter protein NRII by direct interaction with the kinase domain of the transmitter module, *Biochemistry 39*, 13450−13461.
16. Jiang, P., and Ninfa, A. J. (1999) Regulation of the autophosphorylation of *Escherichia coli* NRII by the PII signal transduction protein, *J. Bacteriol. 181*, 1906−1911.
17. Pioszak, A. A., and Ninfa, A. J. (2003) Genetic and biochemical analysis of the phosphatase activity of *Escherichia coli* NRII (NtrB) and its regulation by the PII signal transduction protein, *J. Bacteriol. 185*, 1299−1315.

18. Marina, A., Mott, C., Auyzenberg, A., Hendrickson, W. A., and Waldburger, C. D. (2001) Structural and mutational analysis of the PhoQ histidine kinase catalytic domain: insight into the reaction mechanism, *J. Biol. Chem. 276*, 41182−41190.
19. Tomomori, C., Tanaka, T., Dutta, R., Park, H., Saha, S. K., Zhu, Y., Ishima, R., Liu, D., Tong, K. I., Kurokawa, H., Qian, H., Inouye, M., and Ikura, M. (1999) Solution structure of the homodimeric core domain of *Escherichia coli* histidine kinase EnvZ, *Nat. Struct. Biol. 6*, 729−734.
20. Bilwes, A. M., Alex, L. A., Crane, B. R., and Simon, M. I. (1999) Structure of CheA, a signal-transducing histidine kinase, *Cell 96*, 131−141.
21. Atkinson, M. R., and Ninfa, A. J. (1992) Characterization of mutations in the *glnL* gene of *Escherichia coli* affecting nitrogen regulation, *J. Bacteriol. 174*, 4538−4548.
22. Atkinson, M. R., and Ninfa, A. J. (1993) Mutational analysis of the bacterial signal-transducing protein kinase/phosphatase nitrogen regulator II (NRII or NtrB), *J. Bacteriol. 175*, 7016−7023.
23. Ponting, C. P., and Aravind, L. (1997) PAS: a multifunctional domain family comes to light, *Curr. Biol. 7*, R674−R677.
24. Jiang, P., Peliska, J. A., and Ninfa, A. J. (2000) Asymmetry in the Autophosphorylation of the Two-Component System Transmitter Protein Nitrogen Regulator II of *Escherichia coli*, *Biochemistry 39*, 5057−5065.
25. Pioszak, A. A., and Ninfa, A. J. (2003) Mechanism of the PII-activated phosphatase activity of *Escherichia coli* NRII (NtrB): How the different domains of NRII collaborate to act as a phosphatase, *Biochemistry 42*, 8885−8899.
26. Hendrickson, W. A., and Ogata, C. M. (1997) Phase determination from multiwavelength anomalous diffraction measurements, *Methods Enzymol. 276*, 494−523.
27. Otwinowski, Z., and Minor, W. (1997) Processing of X-ray diffraction data collected in oscillation mode, *Methods Enzymol. 276*, 307−326.
28. Terwilliger, T. C., and Berendzen, J. (1999) Automated MAD and MIR structure solution, *Acta Crystallogr. D55*, 849−861.
29. Terwilliger, T. C. (2000) Maximum likelihood density modification, *Acta Crystallogr. D56*, 965−972.
30. Terwilliger, T. C. (2002) Automated main-chain model-building by template-matching and iterative fragment extension, *Acta Crystallogr. D59*, 34−44.
31. Brunger, A. T., Adams, P. D., Clore, G. M., Delano, W. L., Gros, P., Grosse-Kunstleve, R. W., Jiang, J.-S., Kuszewski, J., Nilges, N., Pannu, N. S., Read, R. J., Rice, L. M., Simonson, T., and Warren, G. L. (1998) Crystallography & NMR System: A new software suite for macromolecular structure determination. *Acta Crystallogr. D54*, 905−921.
32. Jones, T. A., Zou, J. Y., Cowan, S. W., and Kjeldgaard, M. (1991) Improved methods for building protein models in electron density maps and the location of errors in these models, *Acta Crystallogr. A47* (Pt 2), 110−119.
33. Collaborative computational project number 4 (1994) The CCP4 Suite: Programs for Protein Crystallography, *Acta Crystallogr. D50*, 760−763.
34. Kraulis, P. J. (1991). MOLSCRIPT: a program to reproduce both detailed and schematic plots of protein structures, *J. Appl. Crystallogr. 24*, 946−950.
35. Fenn, T. D., Ringe, D., and Petsko, G. A. (2003) POVScript: a program for model and data visualization using persistence of vision ray-tracing, *J. Appl. Crystallogr. 36*, 944−947.
36. Nicholls, A., Sharp, K. A., and Honig, B. (1991) Protein folding and association: insights from the interfacial and thermodynamic properties of hydrocarbons, *Proteins: Struct., Funct., Genet. 11*, 281−296.
37. Kamberov, E. S., Atkinson, M. R., Chandran, P., and Ninfa, A. J. (1994) Effect of mutations in *Escherichia coli glnL* (*ntrB*), encoding Nitrogen Regulator II (NRII or NtrB), on the phosphatase activity involved in bacterial nitrogen regulation, *J. Biol. Chem. 269*, 28294−28299.
38. Pioszak, A. A., and Ninfa, A. J. (2003) Mechanism of the PII-activated phosphatase activity of *E. coli* NRII (NtrB): How the different domains of NRII collaborate to act as a phosphatase, *Biochemistry 42*, 8885−8899.
39. Higgins, D., Thompson, J., Gibson, T., Thompson, J. D., Higgins, D. G., and Gibson, T. J. (1994) CLUSTAL W: improving the sensitivity of progressive multiple sequence alignment through sequence weighting, position-specific gap penalties and weight matrix choice, *Nucleic Acid Res. 22*, 4673−4680.

BI049474R